HNPS Advances in Nuclear Physics

Vol 23 (2015)

HNPS2015

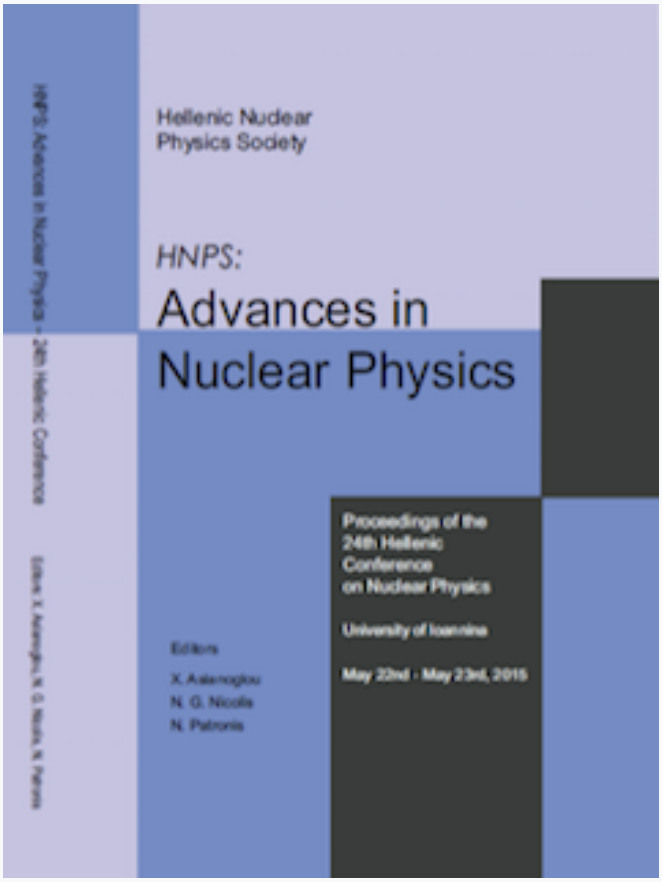

The role of magnetic fields in the formation and propagation of hadronic microquasars jets

E.-D. S. Paspaliaris, T. Smponias, T. S. Kosmas

doi: 10.12681/hnps.1916

Proceedings of the 24th Syposium of the HNPS

The role of magnetic fields in the formation and propagation of hadronic microquasars jets

E.-D. S. Paspaliaris[1,*], T. smponias[1], T. S. Kosmas[1]

[1] *Department of Physics, University of Ioannina, 45110 Ioannina, Greece.*

Abstract

In the present work, we examine the role of the magnetic field (MF), which causes a rather pronounced confinement of the jets at microquasars. Due to radial Lorentz forces acting on the jet's matter towards the jet's axis, the outgoing flux is collimated along the same axis and vertically to the compact object. Alternatively, a rotating central object may drag the surrounding MF into collimation around the produced jet. In such objects, jet emerges from each side of the accretion disc.

These jets operate as cosmic engines, capable of accelerating particles on very high energies ($\sim 10^2$ TeV) and consist sources of high energy neutrinos and gamma rays. We also examine the role of the MF, which causes to a rather pronounced jet confinement. Our aim is to investigate and model its role on various physical observables of the jet, by simulating the jet's flow and derive 2D and 3D visualizations and furthermore examine its effect on the neutrino emissivity.

Keywords hadronic jets, microquasars, magnetic fields, simulation, neutrinos

INTRODUCTION

In general, jets can be produced in binary systems known as microquasars (MQ), being sources of high energy neutrinos and γ-rays, operate as cosmic engines capable of accelerating particles (such as protons, neutrons, pions) on very high energies. The high energy (non-thermal) protons may collide with cold protons leading to the emission of high energy neutrinos and gamma-rays being moderated by the MF [3]. In this work, we have simulated relativistic magneto-hydrodynamic (RMHD) jet flow, for different MF values using the PLUTO hydrocode [9]. By adjusting the relevant physical parameters (injection velocity, pressure and density of the jet), we study the dependence of the collimation of the outflow on the MF (specifically its toroidal component) in and around the jet [7, 10].

Experimenting with different MF values, allowed us to investigate its effect on the neutrino and γ-ray emissivity. We also examined the degree of the jet flow collimation within a chosen region of values of the initial density and injection velocity of the flow [7]. We mainly explored the role of MF in the formation and propagation of jets through 2-D and 3-D animations (using the PLUTO data) produced with Visit 9.1. [10].

* Corresponding author, email: vaggelispaspa@hotmail.com

THEORETICAL DETAILS

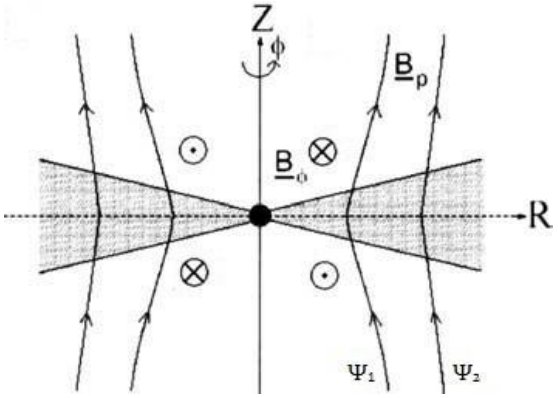

Fig. 1. Schematic view of the two basic components of the magnetic field. The accretion disk is represented by the shaded area around the R-axis. The axis of the jet is the Z-axis [10].

There are two important components of the MF, the toroidal component B_ϕ, along the rotational movement of the accretion disk and the poloidal B_p, along the flow of the jet (Fig. 1). Hence, the MF can be decomposed as,

$$\vec{B} = \vec{B}_p + B_\phi \hat{\phi} \tag{1}$$

The poloidal component can also be expressed as $\vec{B} \equiv \hat{} + B_\phi \hat{\phi}$ In terms of a scalar flux function Ψ, the poloidal equation can be writtenas,

$$\vec{B}_p = \vec{\nabla} \times \left(\frac{\Psi}{r}\hat{\phi}\right) = \frac{1}{r}\vec{\nabla}\Psi \times \hat{\phi} \tag{2}$$

and similarly,

$$\vec{B}_r = -\frac{1}{r}\frac{\partial \Psi}{\partial z}, \quad \vec{B}_z = \frac{1}{r}\frac{\partial \Psi}{\partial r}, \tag{3}$$

while the B_ϕ is independent of the flux function Ψ. The equation of motion for the jet flux is,

$$\rho(\vec{v}\cdot\vec{\nabla})\vec{v} = -\vec{\nabla}P - \rho\vec{\nabla}\Phi + \frac{1}{4\pi}(\vec{\nabla}\times\vec{B})\times\vec{B}. \tag{4}$$

It can also be proved that the poloidal mass flow per unit of poloidal MF is constant along the field lines. The mass load function η, which can be expressed in terms of the flux function Ψ as,

$$\eta(\Psi) = \frac{d\Psi_m}{d\Psi}. \tag{5}$$

Here $d\Psi = \rho u_p dA$ and $d\Psi = B_p dA$ with $u_p \equiv |\vec{u}_p|$ being the poloidal component of the velocity. It can be proved that $\vec{u}_p$ is parallel to the total velocity $\vec{B}_p$, in contrast with the which is not parallel to the total MF [2].

The angular momentum and the energy also relate to the MF as,

$$L(\Psi) = r_A^2 \Omega(\Psi) \tag{6}$$

$$E(\Psi) = \frac{1}{2} v^2 + h + \Phi - \frac{r\Omega B_\phi}{4\pi\eta}, \tag{7}$$

where Ω is the angular velocity, that varies over magnetic surfaces. Equation (7) is the well-known Bernoulli equation for the flow, that expresses the conservation of the energy per unit mass along the poloidal field lines. Function h is the specific enthalpy.

Using equation of motion (4), the Grad-Shafranov equation can also be produced as

$$\nabla \cdot \left[(M_A - 1) \frac{\nabla \Psi}{4\pi r^2} \right] - \left(B_\phi^2 + M_A^2 B_p^2 \right) \frac{\eta'}{4\pi\eta}$$

$$= \rho \left[E' - \Omega_m (\Omega r_A)' - (\Omega_m r^2 - \Omega r_A^2) \Omega' - \frac{\alpha_s^2}{\gamma(\gamma - 1)} K' \right]. \tag{8}$$

The scalar functions (Ψ), (Ψ), Ω(Ψ), $\eta(\Psi)$ and $K(\Psi)$, are integrals of motion that must be prescribed of the boundary conditions and M_A is the Mach-Alfvén number [2].

The rotation of the accretion disk revolves the matter around the central object of the MQ. The acceleration of the jet is supported by the accretion disk which is dominated by a perpendicular MF. The MF lines are stretched by the material that is fixed on the lines (due to the assumption of infinite conductivity), ending up surrounding the jet flow. So, the particles of the ionized material are tight on the lines and behave like beads on a rosary. Due to the initial velocity, the inertia of the flux pushes the MF lines outwards. Finally, the MF becomes highly toroidal and at last helical [4].

In the approximation of a thin disk, the rotation velocity is Keplerian and the effective potential per unit mass is,

$$\Phi_{eff} = -GM_{BH} \left[\frac{r_0}{\sqrt{r^2 + z^2}} + \frac{1}{2} \left(\frac{r}{r_0} \right)^2 \right]. \tag{9}$$

In order to launch the jet, there must be at least one particle to be in unstable equilibrium at the point $(r_0, 0)$. Thus, the second derivative of the effective potential along the MF lines has to be negative.

The collimation of the jet, is achieved by a tensional force associated with B_ϕ leading to a radially inwards directed component of the Lorentz force,

$$F_{L,r} \simeq j_z B_\phi. \tag{10}$$

Due to these (inward pointing) radial Lorentz forces acting on the jet matter towards the jet's central axis, the outgoing flux is collimated along the same axis and vertically to the accretion disk [6]. B_p also contributes to the jet collimation by affecting the minimum opening angle of the jet.

This magneto-hydrodynamic (MHD) theory has to be extended if the flux velocity is comparable with the velocity of light. Under these circumstances Eq. (4) becomes,

$$\rho(\vec{v}\cdot\vec{\nabla})(\xi\vec{v}) = -\vec{\nabla}P - \rho_e\vec{E} + \frac{\vec{J}\times\vec{B}}{c} + \gamma\rho\vec{\nabla}\left(\xi\gamma\frac{GM_{BH}}{\sqrt{r^2+z^2}}\right), \quad (11)$$

where $c^2\xi$ is the relativistic enthalpy per unit mass and γ is the local bulk Lorentz factor of the flux [2].

Angular momentum and energy, are conserved quantities along the poloidal MF lines. In the relativistic case, their expressions are,

$$L(\Psi) = \gamma\xi r v_\phi - \frac{rB_\phi}{4\pi\eta} \quad (12)$$

and

$$E(\Psi) = \gamma\xi\left(\frac{GM_{BH}}{\sqrt{r^2+z^2}}\right) - \frac{r\Omega B_\phi}{4\pi\eta}, \quad (13)$$

respectively [2].

Finally, the shape of the magnetic surfaces emerges from the solution of Eq. (11) for the force balance across the poloidal field lines. Thus, collimation may be achieved through a combination between self-collimation and the pressure by the material that exists around the jet.

RESULTS AND DISCUSSION

In this work, the jet's flow simulations are performed using the PLUTO astrophysical code in its relativistic magneto-hydrodynamic (RMHD) version [1].

Tab. 1. Values of various physical and model parameters for the simulation run [10].

Parameter		Comments
cell size ($\times 10^{10}$cm)	0.25	PLUTO's computational cell
$\rho_{\rm jet}$ (cm^{-3})	1.0×10^{11}	initial jet matter density
$\rho_{\rm sw}$ (cm^{-3})	1.0×10^{12}	stellar wind density
$\rho_{\rm adw}$ (cm^{-3})	1.0×10^{12}	accretion disk wind density
$t_{\rm run}^{\rm max}$ (s)	1.5×10^{3}	model execution time
Interpolation Method	Linear	
Integrator	MUSCL-Hancock	
EOS	Ideal	Equation of state
BinSep (cm)	4.0×10^{12}	Binary star separation
M_{BH}/M_{sun}	3-10	Mass range of collapsed star
M_{star}/M_{sun}	10-30	Mass range of Main Seq. star
$\beta = v_0/c$	0.26	Initial jet speed
$L_{\rm k}^{\rm p}$	2×10^{36}	Jet kinetic luminocity
grid resolution	$120\times200\times120$	PLUTO grid resolution (xyz)

The Generalized Lagrange Multiplier (GLM) correction method is used, enforcing magnetic divergence suppression through hyperbolic divergence cleaning, while the MUSCL-Hancock scheme is employed as the integrator [7]. The stellar wind is set to decrease away from the companion star as $1/r^2$, while a (accretion disk winnd) corona of $1/y^2$, y being the jet axis direction, is setup near the compact object, respectively. The most important model parameters are

shown in Tab. 1 and have been chosen with the purpose to describe the SS-433 system. The VisIt visualization suite is then employed in order to present the results of the simulations in a graphical manner. The boundary conditions are outflow at the top and at the sides of the computational domain ("box") and reflective at the bottom where the jet base is located. The jet's ejection comes from the middle of the bottom (x-z) plane, moving upwards along the model's y- axis.

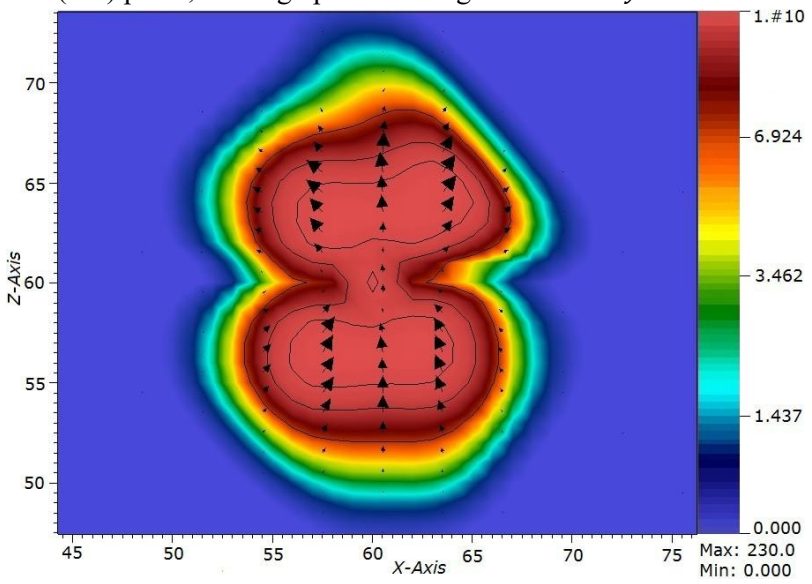

Fig. 2. A 2-dimensional plot of the strongest components of the jet magnetic field, in PLUTO simulation units, for a jet's cross-section, depicting a slice cut parallel to the x-z plane.

The two main components of the MF can be determined, in Fig. 2, and the presence of the toroidal component (ringwise) seems to contribute to the jets confinement through the Lorentz force. The toroidal component of the field is also significant, while other MF lines (vectors) form part of the poloidal component, especially near the jet's central axis. The color shows that the value of the MF is stronger near the same axis.

In Fig. 3 we present three different cases of the same jet's MF magnitude, roughly halfway into the simulation run. As can be seen, if we change the initial value of the MF at the base of the jet, the jet gets a different formation. In case (A), where the initial value is 2G we see that the MF is weak and has cylindrical shape. In case (B), where the value is 50G, we see that the same shape still exists, but now, it is covered by a larger one. The space that is occupied by the MF is larger and its value seems to decrease from the vicinity of the central axis to the outer layers. In case (C), 500G, the MF occupies a somehow smaller volume than in the previous case, but the jet seems to be very well collimated and the magnitude of the MF is stronger, leading to a stronger magnetic force towards the jet axis.

Figure 4 presents the jet's mass density, at the middle of the simulation, for the same cases of the initial MF values, as in Fig. 3. We see that, when the MF is stronger, the jet is more collimated around the central axis. Moreover when the MF takes its lowest value, there is sideways flow and the jet becomes more extended. If we compare Figs. 3 and 4, we conclude that the MF occupies a small portion of the mass density and that explains the sideways flow.

On the otherhand, in cases (B) and (C), the jet is more magnetized and demonstrates a and more focused flow that does not dissipate into the winds.

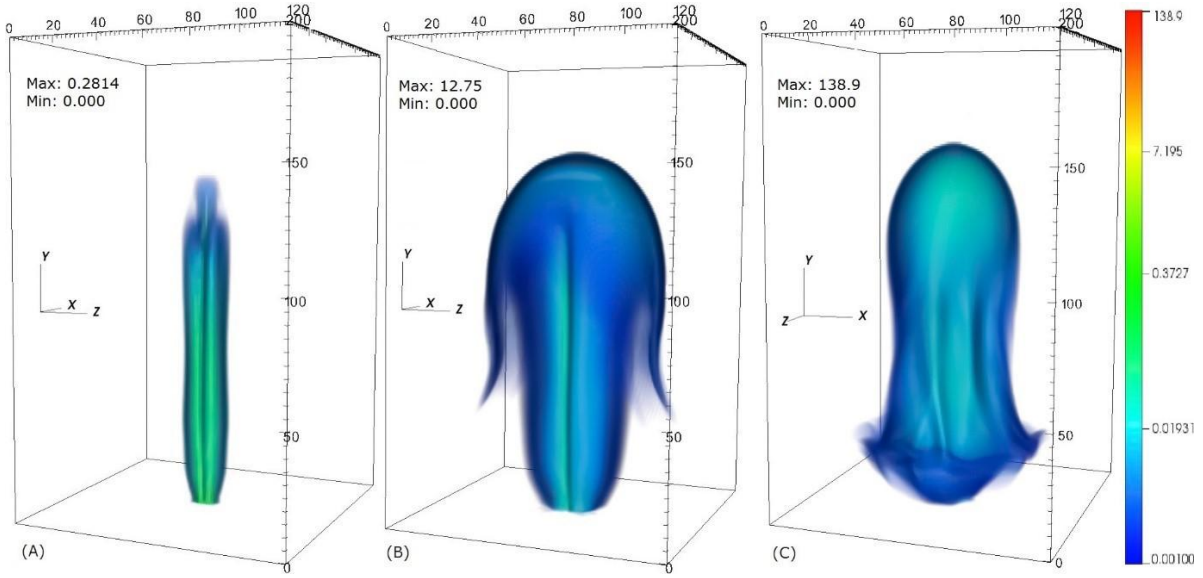

Fig. 3. Plots of the MF magnitude for different MF values at the base of the jet. (A) 2G, (B) 50G, (C) 500G.

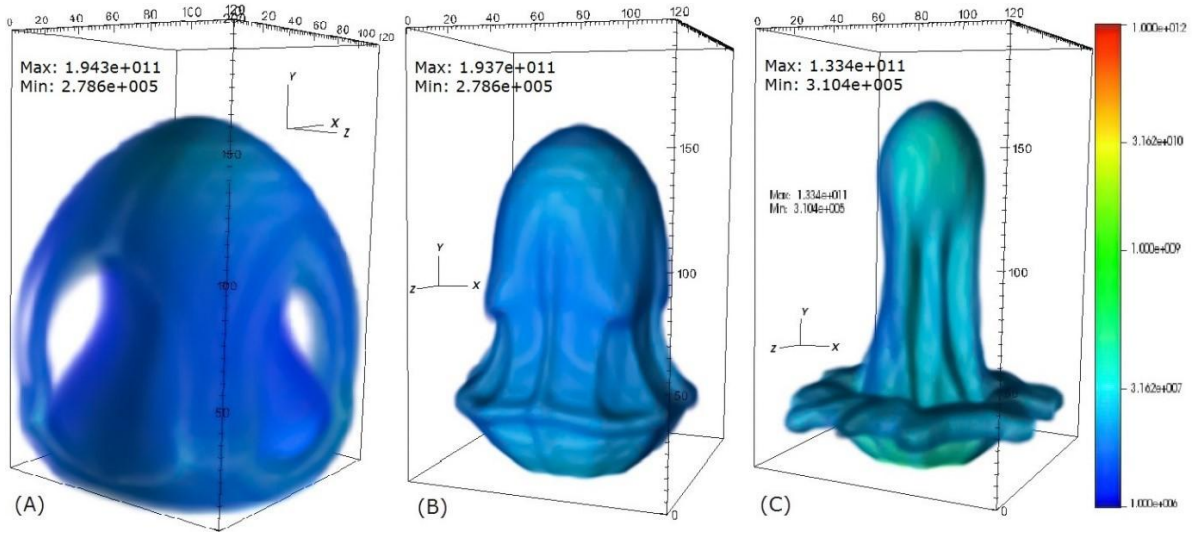

Fig. 4. Plots of the mass density at the jet for different MF values at the base of the jet. (A) 2G, (B) 50G, (C) 500G.

CONCLUSIONS

There is a strong dependence of the jet's collimation on the MF. The confinement of jet flow strongly depends on the magnitude of the toroidal component of the field. This mechanism intensifies the possible neutrino emission, as it allows the magnetized matter to remain dense. At places where the matter density is high, the possibility of the reactions which lead to the neutrino emission is high as well. In this manner, the field contributes to the neutrino emissivity. Moreover, when the MF is strong, the sideways flow is of secondary importance and, therefore, less emission is expected from the sides of the jet. This is opposed

to the weak MF case, where the jet expands more and mixes with the ambient medium, allowing for more dynamical affects to occur over a larger volume at the jet sides. In this case, neutrino emission at vertical directions of the central axis is also expected to occur.

The combination of the results, of the simulations of the jets with theoretical predictions, of the emissivity of neutrinos and the cross sections of p-p and p-γ collisions, using numerical methods, provides detailed investigations of the neutrino production from MQ jets. These methods can also be employed for gamma rays emission estimations of the jets.

References

[1] T. Smponias and T.S. Kosmas, MNRAS **412**, 1320-1330 (2011)
[2] G.E. Romero and G.S. Vila, Lecture Notes in Physcs **876**, (2014)
[3] M.M. Reynoso and G.E. Romero, A&A **493,** 1–11 (2009)
[4] R.D. Blandford and D.G. Payne, MNRAS **192**, 883 (1982)
[5] I.F. Mirabel, C.R. Physique **8,** 7–15 (2007)
[6] R.E. Pudritz, M.J. Hardcastle and D.C. Gabuzda, Space Sci. Rev. **169,** 27-72 (2012)
[7] M. Elizabete, Advances in Space Research **35,** 908–924 (2005)
[8] H.R. Christiansen et. al., Phys. Rev. D73, 63012 (2006)
[9] A. Mignone et al., The Astrophys. J. Suppl. Ser. **170(1)**, 228-242 (2007)
[10] T. Smponias and O.T Kosmas, Adv. High Energy Phys. **2015**, 92757 (2015)